Spatial and Temporal Analysis of Intraperitoneal Chemotherapy Delivery in Heterogeneous Tumor using Multispecies Microbial Ecosystem Modeling

Team 5: Aleysha Chen & Maggie Lin

Abstract

Intraperitoneal (IP) chemotherapy offers a practical advantage for treating peritoneal carcinomatosis by delivering high concentrations of drug directly to tumors in the abdominal cavity. While previous models like that of Rezaeian et al. have explored the impact of vascular heterogeneity and fluid pressure on drug transport, they typically assume a uniform tumor cell population and apply fixed drug concentrations at boundaries. These simplifications may overlook key biological variation that affects treatment outcomes. To address this, we developed a simplified, diffusion-based model that omits pressure-related parameters but includes more biologically realistic features; namely, a Baxter–Jain boundary condition to model drug exchange at the tumor edge and distinct uptake behaviors for sensitive and resistant tumor cell subtypes. Our simulation tracks spatial and temporal variation in drug concentrations and ties this to cell survival over time. We find that resistant cells, which conduct drug uptake more slowly and tolerate higher exposure, tend to persist near the tumor center, while sensitive cells are more effectively eliminated at the periphery. These dynamics suggest that even without convection, spatial differences in drug availability and cellular response significantly influence treatment effectiveness. This work provides a more nuanced view of IP chemotherapy and highlights the role of microenvironmental and cellular heterogeneity in chemoresistance acquisition and tumor evolution.

Background

IP chemotherapy has emerged as a promising locoregional treatment for peritoneal carcinomatosis, enabling direct drug delivery to tumors within the peritoneal cavity shown in Figure 1. A recent image-based mathematical model by Rezaeian et al. provided valuable insights into drug transport during IP chemotherapy by incorporating heterogeneous tumor vasculature and solving convection–diffusion–reaction equations within a reconstructed tumor geometry. However, the model primarily emphasized interstitial fluid pressure (IFP) and fluid flow–driven convection as major determinants of drug penetration, while assuming homogeneous tumor cell populations and uniform pharmacokinetic properties.[1]

This focus, while important, overlooks key biological variability at the cellular level, such as differences in drug internalization between sensitive and resistant tumor cells—factors known to critically influence treatment outcomes. Moreover, the original model applied constant boundary conditions for drug exchange at the vasculature–tumor interface, potentially limiting its accuracy in capturing spatial drug gradients. To address these limitations, we developed a simplified yet biologically enriched model that excludes pressure-related parameters and instead focuses on molecular diffusion, drug–cell binding kinetics, and cellular uptake. Specifically, we implemented the Baxter–Jain boundary condition to model vascular exchange more realistically and introduced distinct internalization rates to simulate differential drug uptake in sensitive versus resistant tumor cells.

Key features of our simulation include spatial drug diffusion, heterogeneous cell population dynamics, and uneven drug distribution. Drug transport is modeled via a mass

transport formulation inspired by the Baxter–Jain model, accounting for capillary-driven release and passive diffusion across the tumor domain. The drug is introduced from a boundary to simulate vascular delivery, creating a concentration gradient that evolves over time.[2] This modified simulation further incorporates two tumor cell types—drug-sensitive and drug-resistant—each characterized by distinct growth rates and drug-induced death thresholds. Cellular behaviors are governed by local drug concentrations, enabling us to simulate selective pressure and competitive interactions in situ. By resolving spatial heterogeneity in drug availability, we capture the emergence of microregions with differential therapeutic exposure. This allows us to study how non-uniform drug penetration drives clonal selection, spatial demixing, and potential treatment failure. This framework allows us to evaluate how cellular-level transport heterogeneity can impact overall drug distribution and treatment efficacy in the absence of bulk fluid flow dynamics.

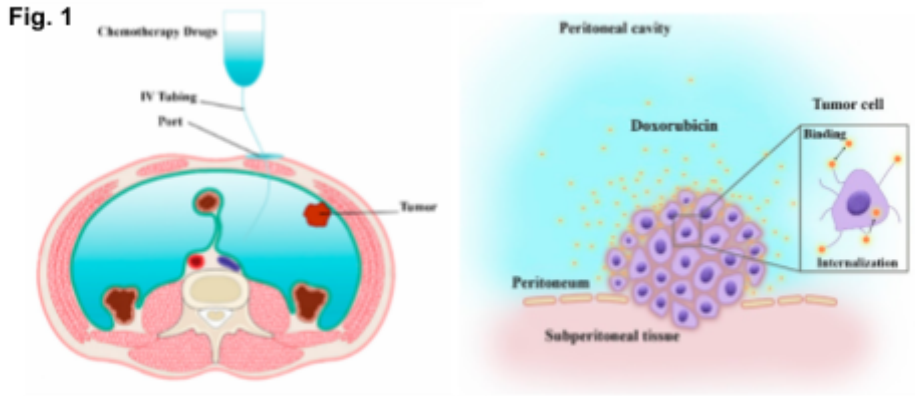

Fig. 1*- Chemotherapy with IP injection shows anti-cancer drugs are delivered directly into the abdominal cavity, where they can penetrate the tumor tissue, bind or unbind to the cancer cells, and finally internalize into the cells. (Image sourced from Rezaeian et al. Cancers, 2023)*

Methods

Procedure 1: Baseline IP drug transport simulation setup

To evaluate drug transport in intraperitoneal (IP) chemotherapy, we first replicated the baseline model presented by Rezaeian et al., incorporating all original parameters related to drug transport, vascular exchange, and binding kinetics—except for those associated with interstitial fluid pressure and convection.[1] This isolates the effects of molecular-level transport and cellular heterogeneity on drug delivery outcomes.

Table 1. Diffusion-dependent IP drug transport model parameters

Parameter	Definition	Unit	Value
S/V	The surface area of blood vessels per unit of tissue volume	m^{-1}	2×10^{4}
k	Hydraulic conductivity of the interstitium	$\mathrm{m}^{2}\cdot\mathrm{Pa}^{-1}\cdot\mathrm{s}^{-1}$	3×10^{-14}

L_P	Hydraulic conductivity of the micro-vascular wall	$m \cdot Pa^{-1} \cdot s^{-1}$	2.10×10^{-11}
σ_s	Average osmotic reflection coefficient for plasma proteins	-	0.9
D_{eff}	Effective diffusion coefficient	$cm^2 \cdot s^{-1}$	3.40×10^{-6}
P	Microvessel permeability coefficient	$cm \cdot s^{-1}$	3.00×10^{-4}
K_{ON}	Constant of binding rate	$M^{-1} \cdot s^{-1}$	1.5×10^{2}
K_{OFF}	Constant of unbinding rate	s^{-1}	8×10^{-3}
K_{INT}	Constant of cell uptake rate	s^{-1}	5×10^{-5}
φ	Tumor volume fraction accessible to drugs	-	0.3
C_{rec}	Concentration of cell surface receptors	M	10^{-5}
ω	Cancer cell survival constant	$m^3 \cdot mol^{-1}$	0.6603

$$\frac{\partial C_F}{\partial t} = -v_i \nabla C_F + D_F \nabla^2 C_F - \frac{1}{\varphi} K_{ON} C_{rec} C_F + K_{OFF} C_B + \Phi \quad \textit{(Eq. 1)}$$

where C_F and C_B (mol/m3) express the free and bound drug concentration in the interstitium, C_{rec} stands for the cell surface receptors' concentration, K_{ON} and K_{OFF} (1/s) are the association and dissociation rate of the drug agents to cell receptors, respectively. D_F (m^2/s) is the therapeutic agents' diffusion coefficient and φ is the volume fraction of the tumor accessible to the drug. Φ is a source term demonstrating drug exchange among microvessels, interstitium, and lymph system, which can be derived as

$$\Phi = \Phi_B - \Phi_L \quad \textit{(Eq. 2)}$$

Φ_L represents the sink term for drug concentration caused by the lymphatic system, which is negligible because the tumor lacks a functional lymphatic system. Also, Φ_B is the drug concentration source provided by microvessels:

$$\Phi_B = (\Phi_B(1 - \sigma_f)C_P + \frac{PS}{V}(C_P - C_F)\frac{P_e}{e^{P_e} - 1}) \quad \textit{(Eq. 3)}$$

where σ_f, C_P (mol/m^3), and *P* (m/s) are the filtration reflection coefficients for the drug, injected drug concentration into the microvessels, and vessel wall permeability. Peclet number, P_e, which reflects the ratio of mass transport via advection to drug transport along microvessel walls, is as follows:

$$P_e = \frac{\Phi_B(1-\sigma_f)}{P\frac{S}{V}}$$ *(Eq. 4)*

The concentrations of the drug that is bound and subsequently internalized are computed as follows:

$$\frac{\partial C_F}{\partial t} = \frac{1}{\varphi}K_{ON}C_{rec}C_F - K_{OFF}C_B - K_{INT}C_B$$ *(Eq. 5)*

$$\frac{\partial C_I}{\partial t} = K_{INT}C_B$$ *(Eq. 6)*

where C_B and C_I represent bound and internalized drug concentrations. In addition, K_{INT} is a constant that represents the internalization rate of the drug into cellular space.

The treatment efficacy, indicated by the fraction of killed cells (FK), is computed for Doxorubicin as follows:

$$FK = 1 - exp(-\omega \times C_I)$$ *(Eq. 7)*

in which ω is a fitting parameter that was obtained from the experiment.

Procedure 2: Incorporate heterogeneous tumor cell population dynamics

To capture intratumoral cellular heterogeneity, we introduced two biologically relevant modifications to the baseline model. First, we incorporated tumor cell population dynamics by modeling two distinct cell types: sensitive (S) and resistant (R) cells. These subpopulations differ in their response to chemotherapy, primarily in terms of drug internalization rates and cytotoxic susceptibility.[3–5]

Each cell population was governed by logistic growth equations with drug-induced death terms dependent on the intracellular drug concentration C_I. Sensitive cells were assigned a higher drug internalization rate (K_{INT}) compared to resistant cells, reflecting differential cellular responses to treatment.

The governing equations for sensitive and resistant cell populations are:

Sensitive Cells

$$\frac{\partial N_S}{\partial t} = -\left(\frac{C_I}{\omega_S x\, 10^{-6}}\right) N_S$$ *(Eq. 8)*

This term represents drug-induced cell death, which increases with intracellular drug concentration C_I and is scaled by a sensitivity constant ω_S. In this equation, the population of sensitive cells is governed by two opposing effects: proliferation limited by space (logistic growth), and reduction due to cytotoxic effects of the internalized drug. (Table 2)

Then follow with the resistant cells:

$$\frac{\partial N_R}{\partial t} = -\left(\frac{C_I}{\omega_R x\, 10^{-6}}\right) N_R$$ *(Eq. 9)*

where the variables are the same, but apply to resistant cells, which typically have lower drug concentration C_I due to slower uptake and higher ω_R, indicating lower sensitivity to drug-induced death. As a result, resistant cells grow more slowly and are less likely to be eliminated by the drug compared to sensitive cells. (Table 2)

Table 2. Sensitive and resistant cell population parameters

Parameter	Definition	Unit	Value
N_S	Population of sensitive tumor cells	cell density	—
N_R	Population of resistant tumor cells	cell density	—
C_I	Intracellular drug concentration	M	—
ω_s	Survival constant of sensitive cells	$cm^3 \cdot mol^{-1}$	6.603×10^5
ω_R	Survival constant of resistant cells	$cm^3 \cdot mol^{-1}$	6.603×10^6

Procedure 3: Incorporate drug diffusion dynamics and realistic drug exchange boundary conditions

Second, to simulate drug distribution within the tumor tissue, we implemented Fick's second law of diffusion, which accounts for both spatial and temporal concentration gradients of free drug in the extracellular space:

$$\frac{\partial D}{\partial t} = D_{eff} \bigtriangledown^2 D \qquad \textit{(Eq. 10)}$$

This term describes the spread of drug via passive diffusion, wherein the loss of drug concentration (D) is directly tied to uptake by cells.

To simulate drug exchange at the tumor–vasculature interface, we applied the Baxter–Jain boundary condition, which captures the limited permeability of the tumor vasculature. This condition ensures realistic modeling of drug extravasation.[2]

Continuity of concentration at the boundary is assumed:

$$C_{tumor} = C_{normal} \qquad \textit{(Eq. 11)}$$

Continuity of flux is defined by:

$$\Phi_{tumor} D_{tumor} \bigtriangledown C_{tumor} = \Phi_{normal} D_{normal} \bigtriangledown C_{normal} \qquad \textit{(Eq. 12)}$$

This formulation enables simulation of spatially continuous diffusion between tumor and surrounding tissue while accounting for differences in tissue porosity and permeability (Table 3). Initial conditions, including starting available dosage (1μM) in plasma, initial tumor density (normalized between 0 and 1), and proportions of sensitive vs. resistant subpopulations are included in Table 4.

Table 3. Baxter-Jain boundary condition parameters

Parameter	Definition	Unit	Value
C_{tumor}	Drug concentration in tumor at tumor-normal tissue interface	M	—
C_{normal}	Drug concentration in normal tissue at tumor-normal tissue interface	M	—
Φ_{tumor}	Volume fraction (porosity) of tumor accessible to drug	—	0.3
Φ_{normal}	Volume fraction (porosity) of normal tissue accessible to drug	—	0.8

Table 4. Initial conditions

Parameter	Definition	Unit	Value
D_F	Free drug concentration in plasma	M	1×10^{-6}
N_0	Initial tumor cell density	—	0.5
f_S	Fraction of tumor cells that are sensitive	—	0.7
f_R	Fraction of tumor cells that are resistant	—	0.3

Results

Diffusion-simplified replication of intraperitoneal drug delivery model

Within the intraperitoneal (IP) chemotherapy model developed by Rezaeian et al., the group explored heterogeneity in vasculature transport of fluid and drug within tumors, modeling the vascular network with a geometry of inlets and outlets. Although this observed a dynamic field of interstitial fluid pressure, highly concentrated within the center of the tumor, this modified

model aims to investigate intratumoral drug transport and its effects on the survival of different cell populations within a heterogeneous tumor.

To focus on the Fickian diffusion involved in IP drug delivery, we replicated a simplified, diffusion-dependent version of the model. Despite observing minimal cell killing, the simulation saw a logistic-like increase in bound drug concentration and a more gradual, linear increase in intracellular drug uptake, similar to the original, pressure-driven model (Fig. 2A).[1] Interestingly, our replication observed a high accumulation of drug levels towards the center of the tumor, which is likely due to the absence of vascular outflow and higher interstitial fluid pressure that would otherwise promote drug extravasation and act as a sink against drug inflow in this simplification.[6–8] This further lends to observing a steady, but minute, increase in cell kill fraction over time at the tumor center that dominates average measurement of cell death across the tumor area (Fig. 2B).

Fig. 2

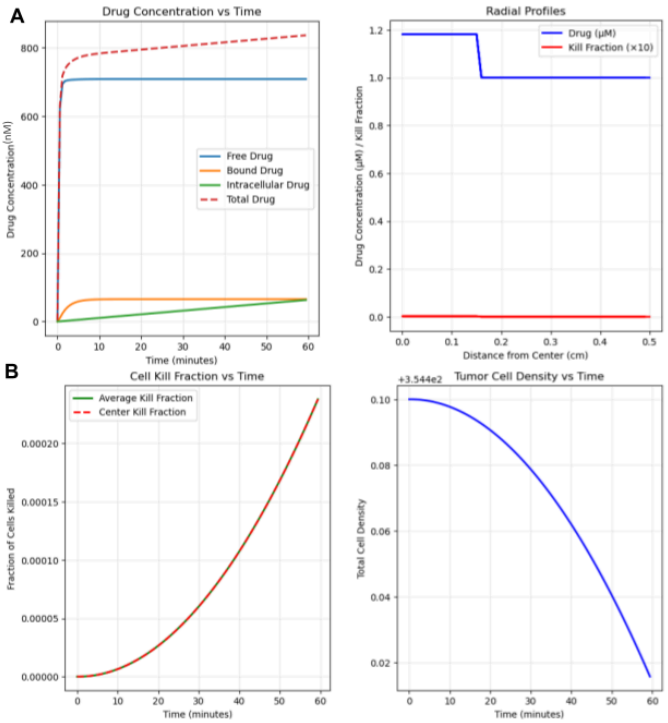

Fig. 2- (A) *Temporal and spatial analysis of change in total, free, bound, and intracellular drug concentrations and fractions of tumor cells killed.* ***(B)*** *Temporal analysis of change in fraction of tumor cells killed and tumor cell density.*

Simulation of IP drug delivery in heterogeneous tumor with Baxter-Jain boundary conditions

As the original model only considered a constant drug concentration at the tumor-normal tissue interface, this modified model implemented a more realistic boundary condition, which mimics that of a tumor surrounded by normal tissue that resorbs fluid excreted by the tumor. This creates a boundary with continuous drug concentration and flux across the tissue interface, reflecting a greater level of drug uptake and more dynamic concentration gradient near the tumor periphery (Fig. 3A).

To simulate cellular heterogeneity in the tumor, reflective of chemoresistance development and treatment evasion acquired with tumor microenvironment interactions, this model stratifies the simulated tumor into drug-”sensitive” and “resistant” subpopulations at

different compositions.[9–11] Although both subpopulations experience similar rates of decrease in cell density with increased distance from the tumor center, likely due to greater cell killing towards the periphery, sensitive cells observe greater fractions of cell death compared to resistant cells (Fig. 3B). This directly reflects the difference in cell survival between the two subpopulations, wherein resistant cells have been previously observed to be relatively at least 10 times more likely to survive treatment exposure than sensitive tumor cells.[3–5]

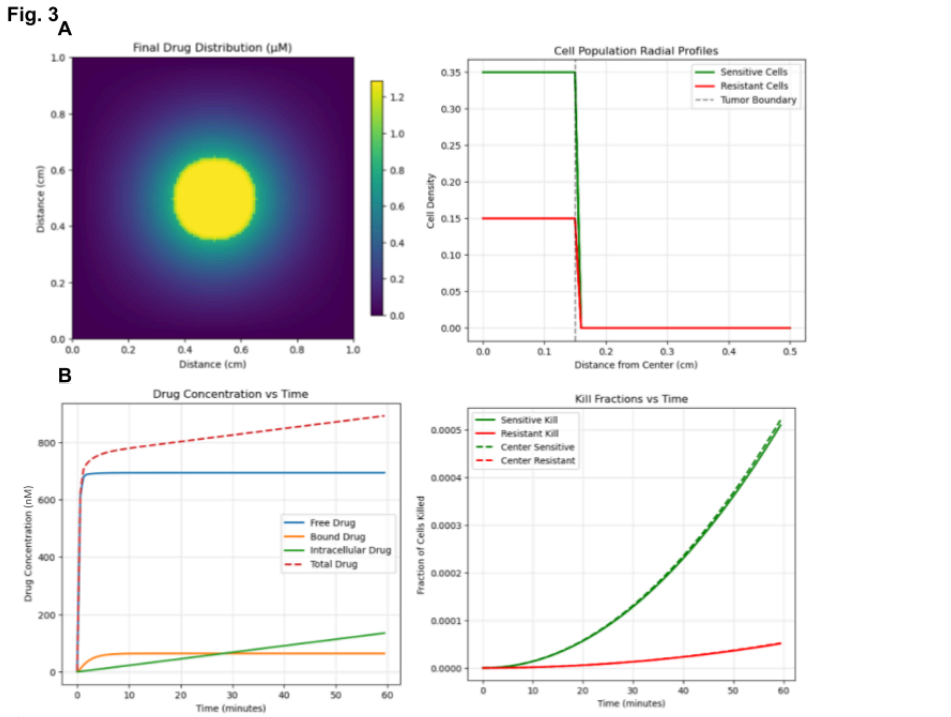

Fig. 3- (A) *Spatial analysis of change in drug concentration and sensitive vs. resistant tumor cell density in response to drug exposure.* ***(B)*** *Temporal analysis of change in total, free, bound, and intracellular drug concentrations and fraction of tumor subpopulations killed.*

Discussion

The modified simulation of IP chemotherapy delivery takes a diffusion-dependent approach, nuanced with a more realistic boundary condition, reflective of dynamic drug concentration at the tumor-normal tissue interface, and a composition of heterogeneous cell types with different drug sensitivity levels. In comparison to the diffusion-dependent simulation with the original model's parameters, the simulation enhanced with the Baxter-Jain boundary condition and heterogeneous tumor composition clearly depicts a more dynamic and realistic representation of spatial and temporal profiles of drug concentration and tumor cell viability.

Specifically, the enhanced model simulated a stratification between the fractions of cell death occurring in the sensitive and resistant subpopulations within the tumor, providing a more granular understanding of the overarching increase in cell killing across time and tumor depth (Fig. 4A). Moreover, while the simplified, diffusion-dependent model observed a slight decrease in drug concentration with increasing distance from the tumor center, saturating at 1uM, implementation of the Baxter-Jain boundary condition in the enhanced simulation saw a continuous decrease in drug concentration with growing distance from the tumor center, reflective of continuous flux at the tumor-normal tissue interface (Fig. 4B). Although these

models are unhindered by vascular pressure and depict an ideal, continuous accumulation of chemotherapy within the tumor core, the dynamic change in drug concentration at the tumor peripheral boundary reflects realistic continuous concentration gradient at the periphery and can be directly applied to existing IFP-driven simulations of IP drug delivery.[6,12–14]

Fig. 4

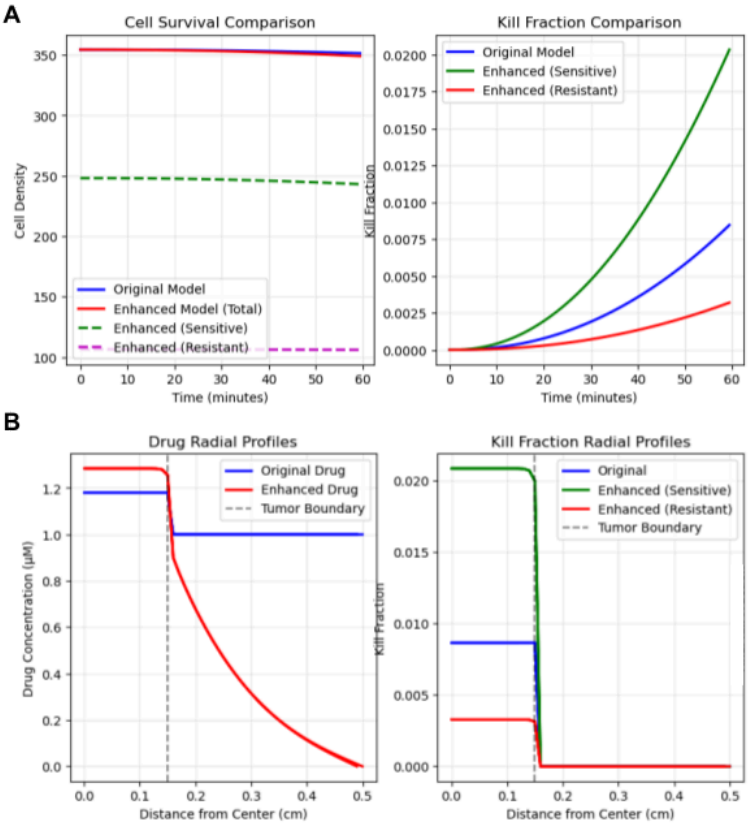

Fig. 4- (A) *Comparative temporal analysis of change in cell survival and fraction of tumor cells killed from drug exposure, between original and enhanced models.* ***(B)*** *Comparative spatial analysis of change in drug concentration and fraction of cell death in tumor subpopulations, between original and enhanced models.*

Code availability

All code used to simulate models and generate plots can be found at: https://github.com/AleyshaC-ucsd/BENG_227_Team_5.

References

1. Rezaeian M, Heidari H, Raahemifar K, Soltani M. Image-Based Modeling of Drug Delivery during Intraperitoneal Chemotherapy in a Heterogeneous Tumor Nodule. Cancers (Basel). 2023 Oct 20;15(20):5069. doi: 10.3390/cancers15205069.

2. Baxter LT, Jain RK. Transport of fluid and macromolecules in tumors. I. Role of interstitial pressure and convection. *Microvasc Res*. 1989;37(1):77-104. doi:10.1016/0026-2862(89)90074-5

3. Mpekris F, Baish JW, Stylianopoulos T, Jain RK. Role of vascular normalization in benefit from metronomic chemotherapy. *Proc Natl Acad Sci*. 2017;114(8):1994-1999. doi:10.1073/pnas.1700340114

4. Mirzayans R, Andrais B, Scott A, Tessier A, Murray D. A sensitive assay for the evaluation of cytotoxicity and its pharmacologic modulation in human solid tumor-derived cell lines exposed to cancer-therapeutic agents. *J Pharm Pharm Sci Publ Can Soc Pharm Sci Soc Can Sci Pharm*. 2007;10(2):298s-311s.

5. McDermott M, Eustace A, Busschots S, et al. In vitro Development of Chemotherapy and Targeted Therapy Drug-Resistant Cancer Cell Lines: A Practical Guide with Case Studies. *Front Oncol*. 2014;4. doi:10.3389/fonc.2014.00040

6. Steuperaert M, Debbaut C, Segers P, Ceelen W. Modelling drug transport during intraperitoneal chemotherapy. *Pleura Peritoneum*. 2017;2(2):73-83. doi:10.1515/pp-2017-0004

7. Choi IK, Strauss R, Richter M, Yun CO, Lieber A. Strategies to Increase Drug Penetration in Solid Tumors. *Front Oncol*. 2013;3:193. doi:10.3389/fonc.2013.00193

8. Dewhirst MW, Secomb TW. Transport of drugs from blood vessels to tumour tissue. *Nat Rev Cancer*. 2017;17(12):738-750. doi:10.1038/nrc.2017.93

9. Quail DF, Joyce JA. Microenvironmental regulation of tumor progression and metastasis. *Nat Med*. 2013;19(11):1423-1437. doi:10.1038/nm.3394

10. Newman AM, Liu CL, Green MR, et al. Robust enumeration of cell subsets from tissue expression profiles. *Nat Methods*. 2015;12(5):453-457. doi:10.1038/nmeth.3337

11. Thibault B, Castells M, Delord JP, Couderc B. Ovarian cancer microenvironment: implications for cancer dissemination and chemoresistance acquisition. *Cancer Metastasis Rev*. 2014;33(1):17-39. doi:10.1007/s10555-013-9456-2

12. Löke DR, Helderman RFCPA, Franken NAP, et al. Simulating drug penetration during hyperthermic intraperitoneal chemotherapy. *Drug Deliv*. 2021;28(1):145-161. doi:10.1080/10717544.2020.1862364

13. Steuperaert M, Falvo D'Urso Labate G, Debbaut C, et al. Mathematical modeling of intraperitoneal drug delivery: simulation of drug distribution in a single tumor nodule. *Drug Deliv*. 2017;24(1):491-501. doi:10.1080/10717544.2016.1269848

14. Soltani M, Chen P. Numerical modeling of fluid flow in solid tumors. *PloS One*.

2011;6(6):e20344. doi:10.1371/journal.pone.0020344